Investigation the polyethersulfone interleaved Glass/Carbon hybrid composite under impact and its comparison with GLARE

Sakineh Fotouhi[1], Joseph Clamp[2], Amir Bolouri[2], Thomas R. Pozegic[3], Mohamad Fotouhi[2*]

[1] Department of Mechanical Engineering, University of Tabriz, Tabriz, Iran

[2] Department of Engineering Design and Mathematics, University of the West of England (UWE), Bristol, BS16 1QY, UK

[3]Bristol Composites Institute (ACCIS), University of Bristol, BS8 1TR Bristol, United Kingdom

Abstract

A tough polyethersulfone (PES) membrane was utilized as a novel reinforcement to improve impact performance of a carbon/glass hybrid composite. The hybrid composite was made of a glass fibre/epoxy block that was sandwiched between two carbon fibre/epoxy blocks. The PES reinforced hybrid composite was compared with an unmodified hybrid composite and a glass reinforced aluminium (GLARE) laminate. During impact testing, results showed that incorporation of PES led to an increase in toughness with a reduction in damage propagation in the investigated composite panels. Furthermore, the results showed that for low impact energy levels (6 J, 12 J and 18 J), the addition of the PES membrane reduced the area of damage by an average of 67%, compared to the virgin laminate. By increasing the impact energy level (24 J and 32 J), fibre breakage was the dominant failure mode and the PES had a negligible effect on the impact performance. A comparable load bearing performance was observed with the hybrid composites and the GLARE laminate for the low energy levels (6 J, 12 J and 18 J). However, the GLARE laminate had a better performance during high energy impacts (24J and 32 J), due to the high ductility of the aluminium plates.

Keywords: Interleaving, Glass/Carbon hybrids, Impact, GLARE, PES

1. Introduction

Poor impact performance is a major drawback for wider application of laminated composite materials. Barely visible impact damage (BVID) severely reduces composite materials' mechanical

capacities, subsequently, it is necessary to consider the presence of this damage at the design stage [1]. Research has previously been carried out to characterize and evaluate the effective parameters in the design of impact resistant composites [2-4]. During low-velocity impact of laminated composites, three main damages mechanisms have been highlighted in the literature: intra-ply cracking, delamination and fibre failure [5]. Delamination is the most common failure mode in laminated composite materials [6].

There have been radical proposals to reduce delamination of composites to improve impact performance of composite laminates. These include: matrix toughening [7], optimization of stacking sequence [8], laminate stitching [9, 10], braided fabric [8], edge cap reinforcement [11], critical ply termination [12], and replacement of a stiff ply by a softer ply [2]. Use of these techniques to arrest delamination leads to weight and cost increase or reduces in-plane mechanical properties. A promising method, to mitigate these problems, is interleaving the ply interfaces with ductile materials to improve the toughness and reduce delamination. Interlayer toughening can be described as the addition of discrete layers of a secondary ductile material between the plies. The aforementioned ductile materials can be categorized into particles - such as micro and nanoparticles - and films - such as thermoplastic Nanofibres mats [13-26]. Studies have shown that fracture toughness improvement in the interleaved laminates improves the impact performance and enhances the residual strength of composite materials. The increased toughness in these composites was attributed to different factors, but mainly inhibiting fibre breakage and pull-out that typically accompanies composite crack growth during impact. However, in order to have an efficient reinforcement, careful consideration is required in the bulk material and reinforcement selection, manufacturing and the cost.

High performance thermoplastics with high modulus and high glass transition temperatures have been reported to be efficient in improving the fracture toughness of laminated composites [27-34]; they can be cured and implemented during the manufacturing process of the laminated composites [35]. One of the constraints of these interleave materials is the requirement of a good chemical and physical compatibility between the interleaving thermoplastic and the bulk thermoset resin. An example of a typical thermoplastic interleaf employed to increase toughness is polyethersulfone (PES). Although PES was reported not to be the most effective additive in improving tensile and flexural properties [36], it still results in significant improvements in fracture toughness [37-39]. PES

forms long molecular chains when bonded with epoxy resin, resulting in increased toughness [39] by inhibiting crack propagation. In optimizing the composite to accommodate PES, Mimura *et al.* [40] studied the effect of different quantities of PES and moulding temperatures on thermal and toughness properties. It was found that with the addition of 10% PES, the glass transition temperature increased by 20 ^{o}C and the toughness increased by 60% compared to an unmodified epoxy. Anthony *et al.* [41] studied the reinforcing effect of PES between the overlapping finger joint regions in pre-cut unidirectional carbon fibre prepreg composites subjected to tension. They reported that addition of the PES interleaf arrested the initial crack which formed at the pre-cut site and delayed catastrophic failure. The strain-to-failure of the PES interleaved samples tested in their publication, increased by 85% compared to the unmodified samples. Subsequently, PES films have demonstrated to have a significant effect on improving fracture toughness of laminated composites [36]. Furthermore, PES is cost-effective and can be implemented easily during manufacturing process of the laminated composites. The onset and propagation of delamination are largely affected by fracture toughness values of composite laminates. A positive correlation is reported between the fracture toughness and impact performance and residual strength of composite materials [42]. Therefore, PES films are a promising addition for composite materials for improving delamination resistance and impact performance of laminated composite materials.

Hybrid composites made of carbon or glass fibre reinforced polymer (GFRP or CFRP) provide synergetic properties, i.e. high strength and light weight of carbon fibre, with the low cost of glass fibre. However, the design of materials and structures becomes a key challenge on how to fully utilize the benefits of these fibres to make a structure strong enough to withstand different loads. Zhu *et al.* [43] investigated the impact behaviour of Ti/M40 fibre reinforced polymer composites. They reported that the fracture performance of hybrid composites was predominately affected by their poor bonding interface. Hung *et al.* [44] studied the mechanical response and failure patterns of carbon/glass fibre reinforced polymer hybrid composites subjected to low-velocity impact with different stacking sequences. It was found that the hybrid composite with surface carbon fibre layers minimised the risk of damage, in terms of the damage size and deflection.

Glass reinforced aluminium (GLARE) laminates are another type of hybrid composite that is widely used for aircraft structures due to its excellent hybrid mechanical properties that are as a result from

mixing the superior fatigue and fracture characteristics of glass fibres, and the plastic behaviour and durability of aluminium metals [45-46]. The impact resistance of a GLARE laminate is related to the aluminium and glass/epoxy properties and is significantly higher than the impact resistance of monolithic aluminium [47]. Similar to other metal-composite interfaces, there is a galvanic corrosion issue, in addition weak strength of the aluminium and glass interfaces in a GLARE laminate causes failure modes such as delamination and debonding [48-56].

A carbon/glass fibre reinforced polymer composite would be a promising alternative for a GLARE laminate, as it would have a lower density, with better fatigue performance than conventional GLARE laminate. This study seeks to improve the low-velocity impact performance of carbon/glass hybrid composites by interleaving with PES membranes and to compare the behaviour with a conventional GLARE laminate. To the authors' best knowledge, PES membranes have not been used to improve impact performance of laminated composite materials. In comparison to other typical interleaves, such as nanofiber electro-spinning, PES membranes, as a method of improving impact resistance of laminated composites, is a cheaper solution due to the low cost of the membranes [27]. This paper has two novel points: the first is the idea of using a PES membrane as impact performance improvement interleave, and the second is to provide a hybrid laminate with a comparable impact behaviour to a GLARE laminate. The interleaf-modified hybrid composites can be developed as modern materials for many engineering applications such as in the aerospace, automotive and civil industries, where high-performance, lightweight and low-cost components are required.

2. Material and methods

Figure 1 illustrates a schematic of the investigated composites and their stacking sequence. For the GLARE sample, a glass/epoxy laminate was sandwiched between two aluminium 2024-T3 sheets. Axiom 3180 glass fibre/epoxy, which is a cross-ply woven prepreg was laid up with stacking sequence of [0/±45/0/±45/0]. The layup was chosen to achieve quasi-isotropic mechanical properties that were found to be most effective in impact by Yaghoubi *et al* [48]. For the hybrid composite and modified hybrid composite plates, two plies of carbon Axiom 5180/epoxy (a cross ply woven prepreg) of [±45/0], were used on each side to replicate both the thickness and the properties of the

aluminium. This is to give a quasi-isotropic material closest to that of aluminium. For the modified hybrid composite, the PES film was laid between the two carbon and glass interfaces with the same stacking sequence of the hybrid composite. A cure of 90 minutes at 130 °C was performed for the GLARE and hybrid composite plates and a cure of 60 minutes at 125 °C was chosen for the modified hybrid composite plate. Table 1 shows thicknesses of the used materials. An attempt was also made to modify interface of the aluminium and glass in the GLARE laminate using the PES film. However, the PES prevented the glass and aluminium from achieving adhesion, despite efforts in trying different surface preparation techniques for the aluminium plate and different curing temperatures.

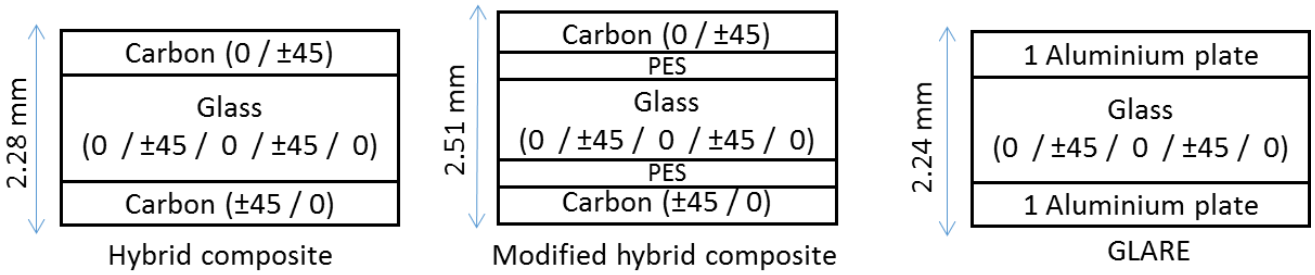

Figure 1. Layup configuration for the investigated samples. Not to scale.

Table 1: Utilised materials and their thickness.

Material	**Thickness (mm)**
Aluminium 2024-T3	0.45
Axiom 3180 Glass fibre/epoxy	0.25
Axiom 5180 Carbon fibre/epoxy	0.25
PES membrane	0.02

The plates were made to be 300 x 300 mm², and then were cut in to 6 pieces of 150 x 100 mm² test samples, in accordance to ASTM D7136 standards [57], in which the laminates with zero angles are oriented along the short edge direction of the sample. Table 2 summarizes the nominal thicknesses and mass for the investigated samples.

Table 2. Mass and thickness of the investigated samples.

Material	Measured cured thickness (mm)	Mass (g) (±0.01)	Mass/m^2 (kg/m^2)
Hybrid composite	2.28	56.64	3.776
Modified hybrid composite	2.51	60.03	4.002
GLARE	2.24	74.43	4.962

3. Testing

The test rig, clamp and the set up were designed based on the ASTM standard D7136 [57] and are illustrated in Figure 2. After centring and clamping the sample, the impactor was raised to the desired height, which was calculated using the gravitational potential energy equation (Energy = mgh, where m = Impactor's mass, h = drop height and g = acceleration due to gravity). Five kinetic energy levels were chosen for a range of impacts, 6 J, 12 J, 18 J, 24 J and 32 J. The 150 x 100 mm² sample was secured over a 125 x 75 mm² hole with four rubber tipped toggle clamps, ensuring no lateral movement. Three samples of each configuration were tested at each energy level with good repeatability. A load cell was positioned underneath the clamped down samples, and consisted of strain gauges. The signal from the gauges was received at 10 kHz and processed through the Strainsmart software. The impactor had a hemispherical tip made from a 12.7 mm ball bearing and is shown in Figure 2-d, preventing sharp edges puncturing the sample and causing additional damage. The total mass of the impactor was 2.82 kg, found by taking ten measurements and averaging the results.

The change in momentum or impulse was calculated by integrating the area under the force time curve. Generating a parabolic trend line to integrate led to a large integration and a less accurate area, so the method was not used, instead, the trapezium rule between each data point gave more accurate area, i.e. Equation 1.

$$\int_{x_0}^{x_n} f(x)\,dx = \frac{1}{2}h[(y_0 + y_n) + 2(y_1 + y_2 + \ldots + y_{n-1})] \quad [1]$$

Where $y_0 = f(x_0)$ and $y_1 = f(x_1)$ etc.

The impact velocity was calculated using the nominal kinetic energy level of each drop, i.e. Equation 2. Calculating the change in momentum, the velocity after impact was calculated using Equation 3, where *v* is the velocity of the impactor, *v'* is the velocity after impact and *m* is the impactor's mass.

$$v = \sqrt{\frac{2KE}{m}} \quad [2]$$

$$v' = \frac{\Delta p}{m} + v \quad [3]$$

Where *v, KE, m* and *p* refer to the impactor's velocity, kinetic energy, mass, and potential energy, respectively.

Finally, having both the initial and final velocities, the change in energy can be calculated using Equation 4. This determines the energy lost in the impact in which most is absorbed by the material. Other energy losses are assumed to be negligible.

$$E_1 = \frac{1}{2}m(v^2 - v'^2) \quad [4]$$

Where E_1, *m* and *v* refer to the energy lost, impactor's mass and velocity, respectively.

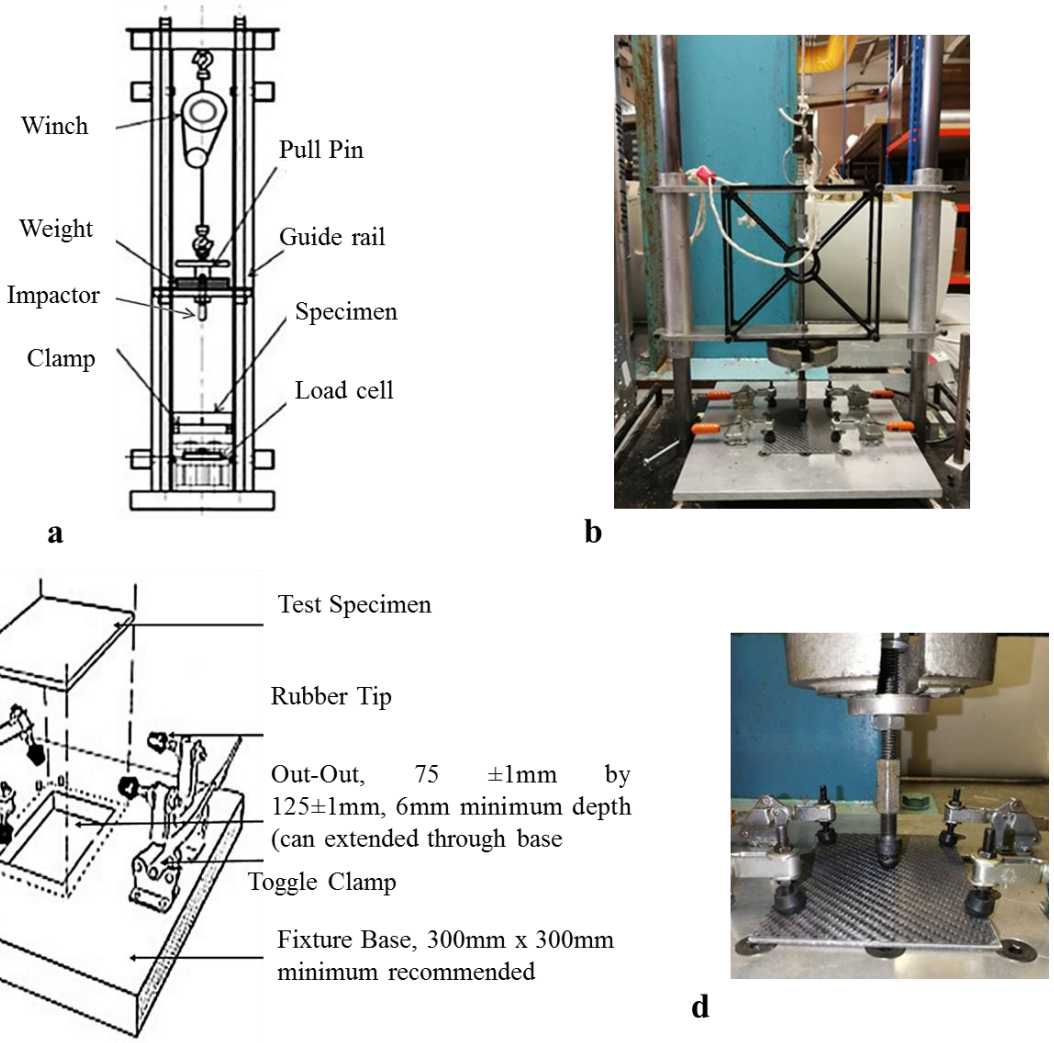

Figure 2. a) Diagram of a low-velocity test rig, b) Low-velocity test rig (impact tower), d) Clamped sample and impactor, and c) ASTM standard clamp and test set up.

4. Results and discussion

Initially, each impact energy level is individually assessed to analyse how the contact force differs for each sample with complementary analysis of cross-sectional micrographic photographs for each impact. Following this, the total impact energy loss is plotted and impact damage area is assessed. The damage assessment of impacted specimens was evaluated by cross-sectional photography analysis, absorbed energy and visual inspection of the surface of the impacted and non-impacted side. The results are summarized as follows.

4.1 Load-time plots and cross-sectional images

Figure 3 shows load-time curves for the impacted samples at different energy levels. Considering the shape of the curves for the force-time results, all the samples demonstrate a linear behaviour in the early stages of the loading process as an elastic response. This is followed by a drop in the contact force owing to the damage caused by the impact. As can be seen from Figure 3, there are some observable differences in the shape of the curves owing to the nature of the damage mechanisms for the investigated samples. There is a secondary peak for the laminates that were penetrated by the impactor for the high impact energy levels tests (24 J and 32 J). The three main quantitative areas for analysis on these graphs are the maximum contact force, the initial gradient and the total impact time. These give key evidence to the materials properties and how the materials behave during impact. As can be seen in Table 2, the GLARE laminate is 31% and 24% heavier than the hybrid composite and the modified hybrid composite, respectively. However, as illustrated in figure 3, all the investigated samples have similar gradients in the force-time plots. The modified hybrid composite and the hybrid composite are slightly steeper initially which is to be expected as the carbon layers add stiffness to the hybrid composites. The investigated samples have identical in-plane dimensions, but the thickness of the modified C/G/C Hybrid laminate (2.51 mm) is 10% and 12% higher than that of the C/G/C Hybrid laminate (2.28 mm) and the GLARE (2.24 mm), respectively. Therefore, in order to have a fair comparison between the impact behaviours, the results were normalized by a thickness scaling rule. Previous publications [58-59] on scaling the low-velocity impact behaviour of composites, with the same in-plane dimensions and different thicknesses, suggest that the load should be scaled as $R^{1.5}$ with the resulting plate time (deflection) remaining the same, where R is the thickness ratio.

Table 3 reports values of the maximum contact force and total impact time for the investigated laminates. The values with an asterisks are the scaled load values, where the thicknesses are scaled to the GLARE thickness (2.28 mm). Comparing the scaled results, the modified hybrid and hybrid composites have higher contact force than the GLARE composite for the low-energy levels (i.e. 6 J and 12 J). However, by increasing the energy level (i.e. to 18J, 24J and 32 J), the GLARE composite

had a higher contact force. Higher contact force means higher load bearing capabilities and high stiffness.

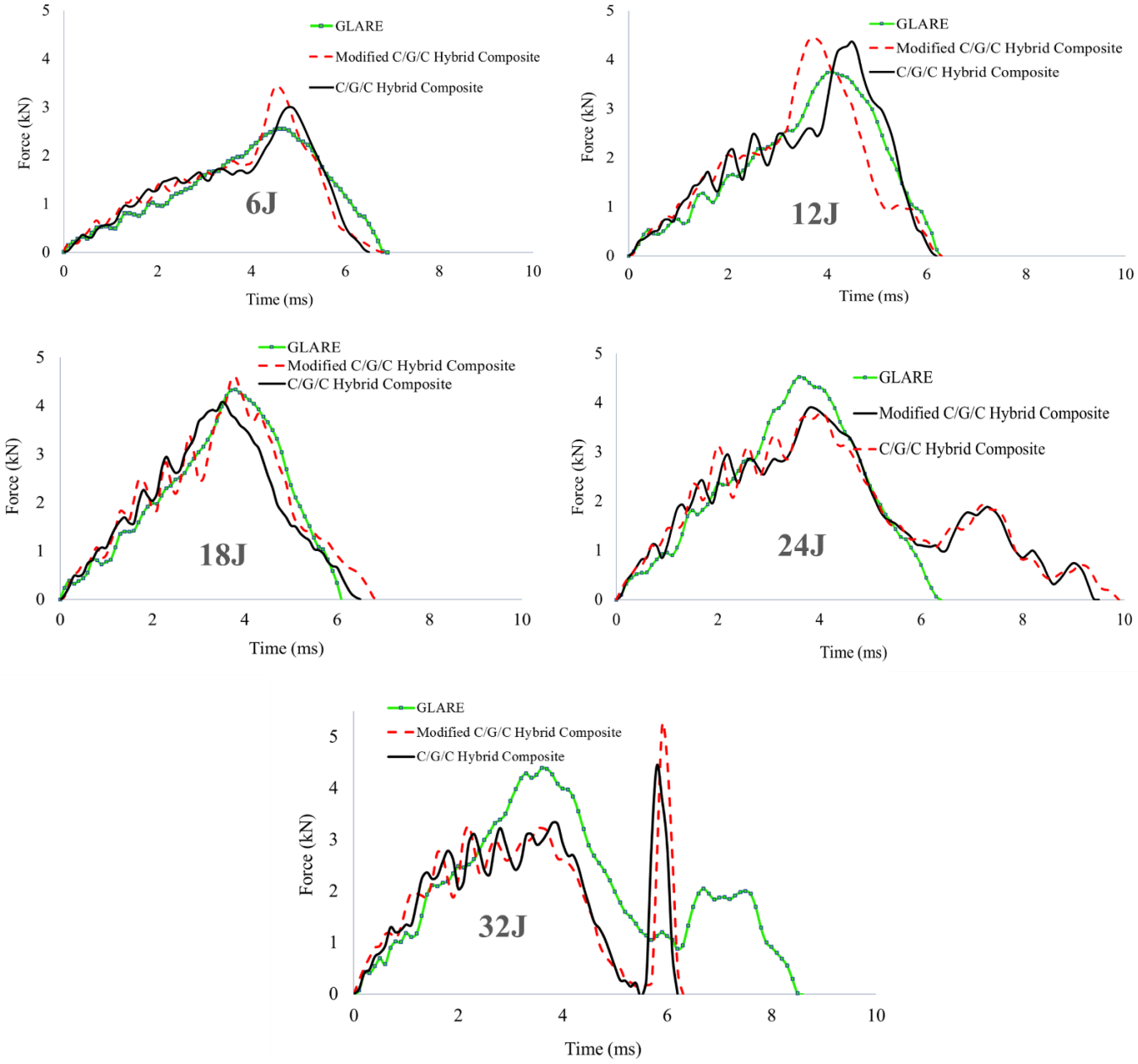

Figure 3. Time development of force for the samples impacted at 6J, 12 J, 18J, 24 J and 36 J.

Table 3. Values of maximum contact force and the total impact time for the impacted samples.

Impact energy level (J):		**6**	**12**	**18**	**24**	**32**
Maximum contact force (kN)	Hybrid composite	3.00 2.92*	4.37 4.25*	4.08 3.97*	3.77 4.07*	3.31 3.22*
	Modified hybrid composite	3.42 2.88*	4.44 3.75*	4.60 3.88*	3.90 3.29*	3.27 2.75*
	GLARE	2.55	3.75	4.34	4.52	4.38
Total impact time (ms)	Hybrid composite	6.5	6.2	6.5	9.5	6.2
	Modified hybrid composite	6.8	6.3	6.9	9.9	6.3
	GLARE	6.9	6.3	6.1	6.4	8.6

* The multiplied quantity of the hybrid and modified hybrid composites with scaling factor.

4.2 Damage analysis

Figures 4-6 show the cross-sectional side view (Fig. 4.), the bottom side view of the non-impacted side (Fig. 5.) and the front side view of the impacted side (Fig. 6) for the different impact energies. For the 6J energy level, bending can be seen on the GLARE sample but no delamination between the aluminium and the glass layers can be observed. Only minor fibre breaks are visible on the back side of the hybrid composite, while no visible damage occurred to the modified hybrid composite. BVID is likely to have occurred in all these three samples, however, the main aim of the cross-sectional photographs is to see visible damage and delamination between the dissimilar interfaces, i.e. the carbon/glass interface and the aluminium/glass interface. At 12 J, damage of the modified hybrid composite and hybrid composite appear very similar, where no apparent delamination has occurred, only fibre fracture on the non-impacted side. The GLARE sample has some delamination between the upper aluminium plate and the glass/epoxy laminates, with visible yielding of the aluminium observable on the impacted and non-impacted faces at the impact point.

At 18J, larger scale damage occurred, compared with 6 J and 12 J, with fibres failing throughout the thickness of the modified hybrid composite and hybrid composite. The GLARE composite experiences significant delamination between the aluminium and the glass in the lower side, but the aluminium layers underwent yielding and denting without rupture. The higher drop in the contact force of the hybrid composites, compared with the GLARE composite (see Figure 3), is attributed to

the observable damage mechanisms with the impact energy being absorbed by these damage mechanisms for the hybrid composites. The damage in the hybrid composite is greater than that in the modified hybrid composite with clear fibre break and disruption on the back face.

At 24 J, both the modified hybrid composite and hybrid composite curves have a second peak in their force-time curves (see Figure 3). This is due to the penetration of the impactor in the composites that causes initial impact breaks through the layers. There is a second increase in the contact force as the lower side fibres stop further penetration of the impactor. Even if there is significant delamination in the GLARE laminate, the contact force in this laminate is still higher than the hybrid composites owing the aluminium that has not completely ruptured. However, on the non-impacted side, the aluminium cracked with a small petaling effect in addition to delamination propagating further from the impact point than during the previous impact. The damage for the hybrid composite samples was more localized than in the GLARE sample.

At 32 J, the impactor fully penetrated both the modified hybrid composite and hybrid composite, becoming impregnated within the sample after the impact. In Figure 3, the curves for the modified hybrid composite and hybrid composite show little initial resistance to the impactor with less than 3.5 kN contact force breaking through the sample. Following this, both curves spike sharply due to the widening of the impactor after the ball bearing, preventing it from passing through the sample completely. The high contact force indicates the high amount of residual energy in the impactor even after it has penetrated the sample. The GLARE sample was also penetrated, but with a higher contact force and lower subsequent spike. The modified hybrid composite and hybrid composite fail catastrophically with fibre failure throughout the impact and some delamination around the impact area. The GLARE however failed in a different way; it cracked with petaling and some fibre failure, but there were substantial amounts of delamination between the aluminium and glass fibre interfaces. The time taken during the impact is also much longer for GLARE, showing more ductility of the aluminium layers.

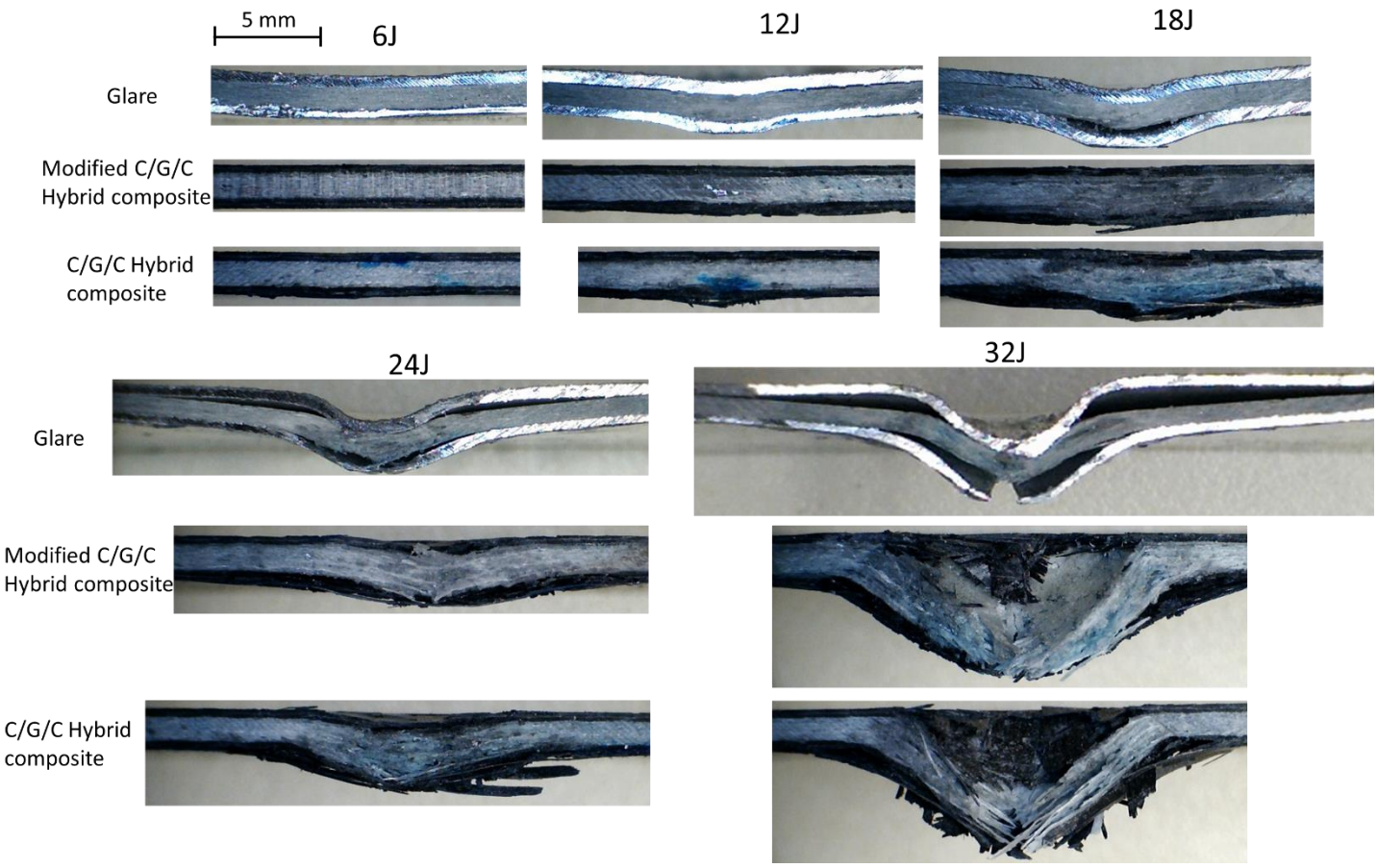

Figure 4. Cross-sectional image of the damaged specimens for different impact energy levels.

1

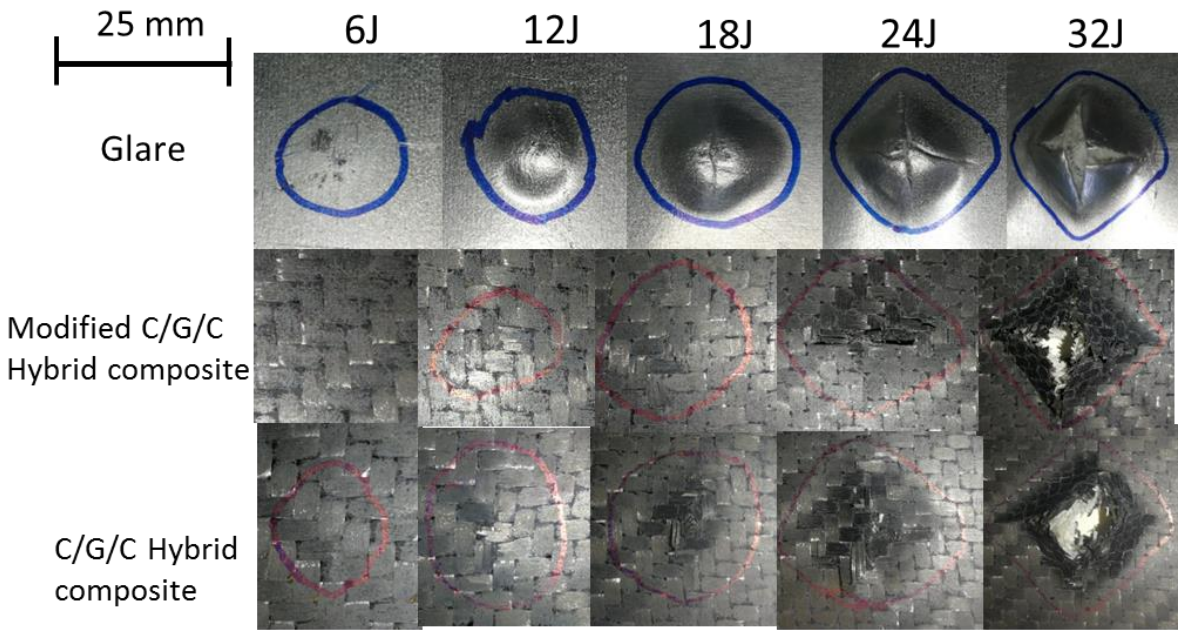

Figure 5. Bottom surface (non-impacted side) view of the investigated samples subjected to different energy levels.

1

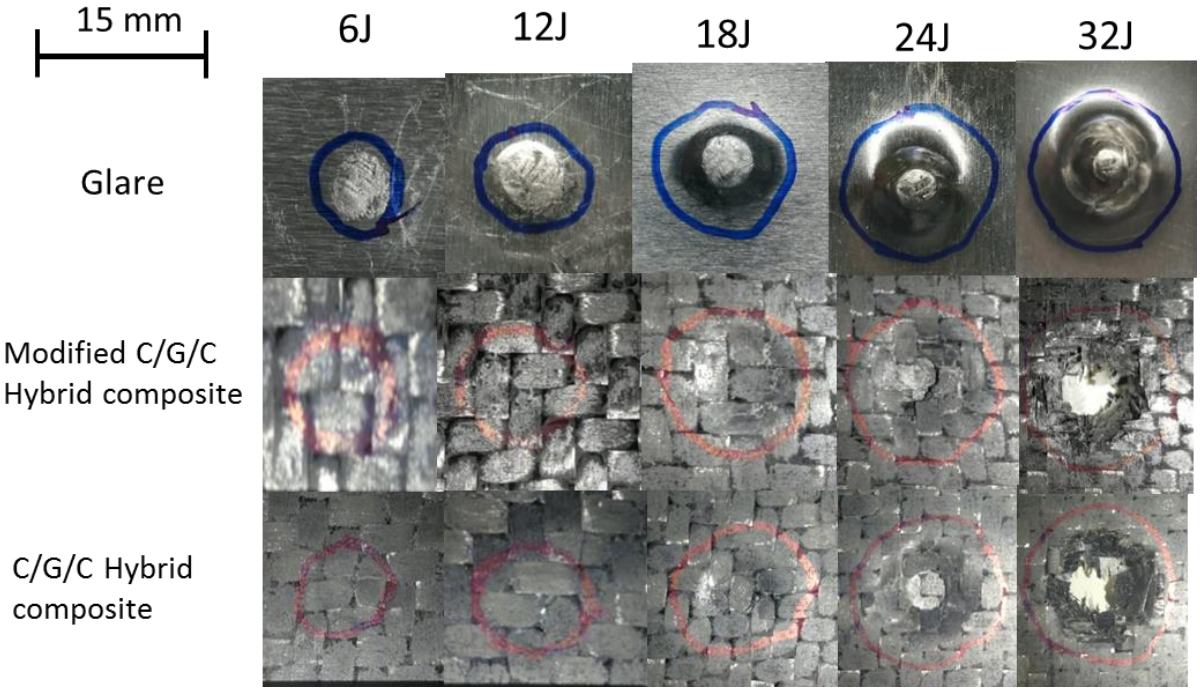

Figure 6. Front surface (impacted side) view of the investigated samples subjected to different energy levels.

4.3 Damage size and absorbed energy

The damage size was assessed through visual inspection of the surface damage illustrated in Figures 5 and 6. To measure the areas, a circle or square was drawn around the damaged area and the diameter or diagonal length measured. To aid comparison, the size of the observable damaged area (measured from both impacted and non-impacted sides) for each impact energy level are presented graphically in Figures 7-8 and are summarized in Table 4. Error lines were applied to the graphs to allow for inaccuracies in the measuring of the areas and irregularities in the shapes i.e. not being a perfect circle or square. Comparing the results in Figures 7 and 8, the damage on the impact side was relatively small and circular, compared with the non-impacted side, where shear band failure and fibre failure resulted in the rhombus pattern. The higher damaged area on the non-impacted side is due to the combination of tension and shear stresses that generated shear dominated damage at the interfaces (delamination) and tension dominated damage (fibre breakage). This observation was similar to previous studies [44, 60], where larger damage was observed in the lowerhalf compared to the upper half, for the polymer fibre composite laminates.

Referring to the four non-penetrative impacts of 6, 12, 18 and 24 J, there are clear patterns in the impacts with the area of damage rising linearly with impact energy. From Table 4, the modified hybrid composite consistently sustained less damage than the hybrid composite in the non-impacted side, with the area being reduced by 100, 65, 35, 19 and 0% for impact energy levels of 6, 12, 18, 24 and 32 J, respectively. In the lowest two impact energies, the damage sustained by the GLARE sample remained almost the same owing to the majority of the damage resulting from the protrusion of the aluminium. The damage then rises linearly, but at a lower rate than both the hybrid samples demonstrating improved impact performance of the GLARE. The penetration during the 32 J impact meant the effect of the PES became negligible leading to the modified hybrid and the hybrid samples sustaining the same area of damage, while the GLARE sample's damage still rose linearly compared to the previous impacts.

Comparing the induced damage in the impacted side, the hybrid sample had more damage in all the energy levels except 12 J. The improvements made by PES are clear in reducing the area of damage by 47, 28, 6 and 5% for 6, 18, 24 and 32 J, respectively.

1

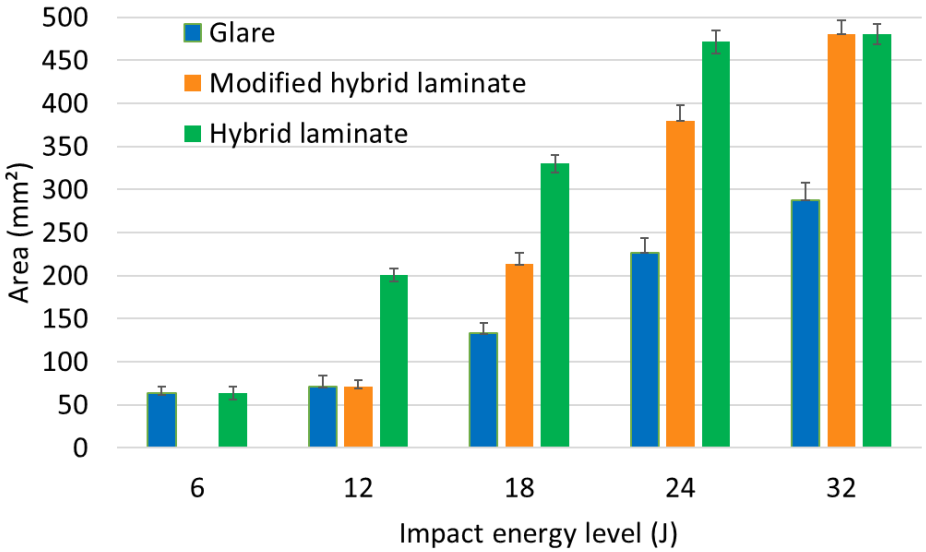

Figure 7. Comparison of the bottom surface damaged area for the investigated samples at different energy levels.

2

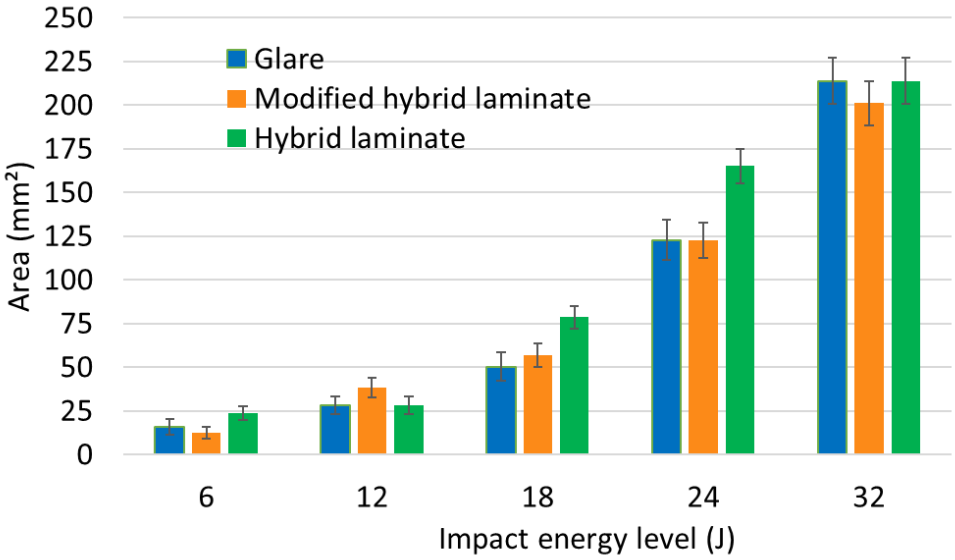

Figure 8. Comparison of the front surface damaged area for the investigated samples at different energy levels.

3

The impact energy loss was calculated using Equation 4. The obtained results are illustrated in Figure 9 and are summarized in Table 4. A direct relationship exists between the damage size and energy loss. As can be seen from the results, for all the energy levels except 24 J (i.e. 6, 12, 18 and 32 J), the energy loss for the investigated samples is similar, even if there is a minor variation. With reference to Figures 4, 5 and 6, at 24 J the GLARE had considerably more energy loss than the modified hybrid composite and hybrid composite - the GLARE sample sustained much less catastrophic damage in this energy level while withstanding a higher contact force. The non-impacted side created a high energy absorbing failure mode.

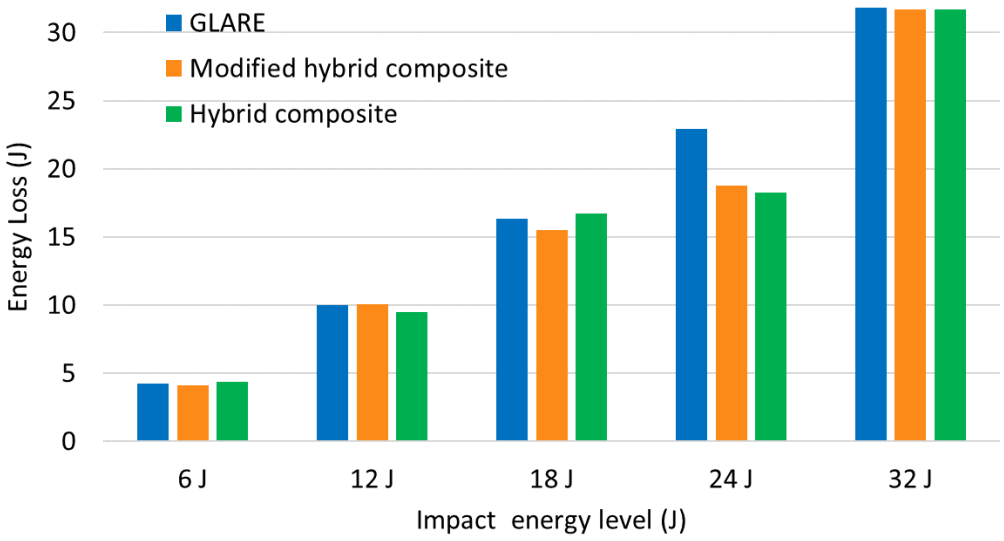

Figure 9. Comparison of the energy loss at different energy levels.

Table 4. Calculated damaged area and energy loss for the investigated samples at different energy levels.

Impact energy level (J):		6	12	18	24	32
Energy loss (J)	Hybrid composite	4.20	9.98	16.74	18.27	31.67
	Modified hybrid composite	4.12	10.06	15.50	18.74	31.67
	GLARE	4.20	9.98	16.35	22.90	31.85
Damaged area (mm^2), impacted side.	Hybrid composite	23.76	28.27	78.54	165.13	213.82
	Modified hybrid composite	12.57	38.48	56.74	122.72	201.06
	GLARE	15.9	28.27	50.26	122.72	213.82

Damaged area (mm^2), Non-impacted side.	Hybrid composite	63.62	201.10	330.06	471.43	480.50
	Modified hybrid composite	0.00	70.88	213.82	380.13	480.50
	GLARE	63.62	70.88	132.73	226.98	288.00

5. Conclusion

This paper studied the effect of PES interleaving as a novel toughening mechanism for carbon/glass hybrid composites when subjected to low-velocity impact. The modified hybrid composites were compared with the unmodified hybrid composite and the GLARE laminate with regards to the load bearing capacity and the associated damage mechanisms. The experimental results showed that for low impact energy levels (6 J, 12 J and 18 J), the addition of the PES membrane reduced the damaged area compared to the unmodified hybrid composite by an average of 67%. However, by increasing the impact energy level (24 J and 32 J), the PES membrane did not have a significant effect on the impact performance. This is a result of observable localized fibre breakage and penetration as dominant damage mechanisms. For the low energy levels (6 J, 12 J and 18 J), a comparable load bearing capacity performance was observed for the hybrid composites and the GLARE laminate. The GLARE laminate had a better performance in the high impact energy levels (24 J and 32 J) owing to ductile and gradual failure of the aluminium plates. It can be concluded that PES interleaving is an efficient way to improve low-velocity impact resistant of hybrid laminated composites by improving delamination resistance between dissimilar interfaces.

References (Needs to be checked)

[1] Safri SNA, Sultan MTH, Yidris N and Mustapha, F. Low velocity and high velocity impact test on composite materials – A review. The International Journal of Engineering and Science (IJES). 2014; 3: 50–60.

[2] Shivakumar K, and Panduranga R. Interleaved polymer matrix composites – a review. North Carolina A&T State University, Greensboro, NC, 27411, USA, 2013.

[3] Hojo M, Matsuda S, Tanaka M, Ochiai S, Murakami A. Mode I delamination fatigue properties of interlayer-toughened CF/epoxy laminates. Compos. Sci. Technol. 2006; 66: 665-675.

[4] Nobuyuki O, Hajime K, Masaki Y. Development of torayca prepreg P2302 carbon fiber reinforced plastic for aircraft primary structural materials. Adv. Compos. Mater. 1996; 5: 249-254.

[5] Saghafi H, Palazzetti R, Zucchelli A, Minak G. Impact response of glass/epoxy laminate interleaved with nanofibrous mats. Eng Solid Mech. 2013; 1: 85–90.

[6] Saeedifar M, Fotouhi M, Ahmadi Najafabadi M, Hosseini H. Prediction of delamination growth in laminated composites using acoustic emission and Cohesive Zone Modeling techniques. Composite Structures 2015; 124: 120-127.

[7] Odagiri N, Muraki T and Obukuro K. Toughness improved high performance Torayca prepreg T800H/3900 series, Proc.33rd Int, SAMPE Symp., Anaheim, CA, 1988; 272-83.

[8] Pagona NJ and Pipes RB. The influence of stacking sequence on laminate strength, Journal of Composite Materials. 1971; 5: 50-57.

[9] Mignery LA, Tan T.M and Sun C.T. The use of stitching to suppress delamination in laminated composites, ASTM STP 876, American Society for testing and materials, 1985; 371-385.

[10] Dow MB and Dexter H.B. Development of stitched, braided of composite structures In the ACT program and Langley research center, NASA TP-97-206234, 1997.

[11] Howard WE, Gossard T and Jones R.M. Reinforcement of composite laminate free-edges with U-shaped caps, AIAA Journal. 1986; 610-62327.

[12] Chan WS and Ochoa OO. Edge delamination resistance by a critical ply termination, Key Engineering Materials. 1989; 37: 258-293.

[13] Robinette EJ. Toughening Vinyl Ester Matrix Composites by Tailoring Nanoscale and Mesoscale Interfaces. PhD Dissertation, Chemical & Biological Engineering Department, Drexel University: Philadelphia, PA, USA, 2006.

[14] Sela N, Ishai O, Interlaminar fracture toughness and toughening of laminated composite materials: A review. Composites 1989; 20: 423-435.

[15] Yun N, Won Y, Kim S. Toughening of epoxy composite by dispersing polysulfone particle to form morphology spectrum. Poly. Bull. 2004; 52: 365-372.

[16] Min H, Kim S. Fracture toughness of polysulfone/epoxy semi-IPN with morphology spectrum. Poly. Bull. 1999; 42: 221-227.

[17] Dzenis Y, Reneker D. Delamination resistant composites prepared by small diameter fiber reinforcement at ply interfaces. US Patent 6265333, 2001.

[18] Sihn S, Kim RY, Huh W, Lee KH, Roy AK, Improvement of damage resistance in laminated composites with electrospun nano-interlayers. Compos. Sci. Technol. 2008; 68: 673-683.

[19] Li G, Li P, Yu Y, Jia X, Zhan S, Yang X and Ryu S. Novel carbon fiber/epoxy composite toughened by electrospun polysulfone nanofibers. Mater. Lett. 2008; 62:511-514.

[20] Li G, Li P, Zhang C, Yu Y, Liu H, Zhang S, Jia X, Yang X, Xue S and Ryu S. Inhomogeneous toughening of carbon fiber/epoxy composite using electrospun polysulfone nanofibrous membranes by in situ phase separation. Compos. Sci. Technol. 2008; 68: 987-994.

[21] Zhang J, Lin T, Wang X. Electrospun nanofibre toughened carbon/epoxy composites: Effects of polyetherketone cardo (PEK-C) nanofibre diameter and interlayer thickness.Compos. Sci. Technol. 2010; 70: 1660-1666.

[22] Liu L, Liang Y, Xu G, Zhang H and Huang Z. Mode I Interlaminar fracture of composite laminates incorporating with ultrathin fibrous sheets. J. Rein. Plast. Comp. 2008: 27:1-15.

[23] Adams JE. Mitigation of Delamination in Polymeric Composites by Polymer Nanofiber Interleaving. PHD Dissertation, Mechanical Engineering Department, A&T State University: Greensboro, NC, USA, 2012.

[24] Ghantae S. Analysis and Mitigation of Effects of Edge Stresses in Multidirectional Fiber Reinforced Composite Laminates. PHD Dissertation, Mechanical Engineering Department, A&T State University: Greensboro, NC, USA, 2012.

[25] Akangah P, Lingaiah S, Shivakumar K. Effect of Nylon-66 Nano-fiber Interleaving on Impact Damage Resistance of Epoxy/Carbon fiber Composite Laminates. Composite Structures. 2010; 92:1432-1439.

[26] Saghafi H, Fotouhi M, Minak G, Saeedifar M. Improvement of the impact properties of composite laminates by means of nano-modification of the matrix-A review, Applied Sciences: Nanotechnology and Applied Nanosciences. 2018; 8(12): 2406.

[27] Fotouhi M, Saghafi H, Brugo T, Minak G, Fragassa C, Zucchelli A, Ahmadi M. Effect of PVDF nanofibers on the fracture behavior of composite laminates for high-speed woodworking machines Proceedings of the Institution of Mechanical Engineers, Part C: Journal of Mechanical Engineering Science. 2017; 231: 31-43.

[28] Brugo T, Minak G, Zucchelli A, Saghafi H, Fotouhi M. An investigation on the fatigue based delamination of woven carbon-epoxy composite laminates reinforced with polyamide nanofibers Procedia Engineering. 2015; 109: 65-72

[29] Brugo T, Minak G, Zucchelli A, Yan XT, Saghafi H, Fotouhi M, Palazzetti R. A study on fatigue behavior of nanointerleaved woven CFRP, European Conference on Composite Materials-ECCM 17, 2016.

[30] Chen SF, Jang BZ, Fracture behaviour of interleaved fiber-resin. Compos. Sci. Technol. 1991; 41: 77-97.

[31] Anand A, Kumar N, Harshe R, Joshi M. Glass/epoxy structural composites with interleaved nylon 6/6 nanofibers. Engineering Solid Mechanics. 2015; 3: 21-26.

[32] Saghafi H, Brugo T, Minak G, Zucchelli A. Improvement the impact damage resistance of composite materials by interleaving Polycaprolactone nanofibers. Engineering Solid Mechanics. 2015; 3: 21-26

[33] Saghafi H, Zucchelli A, Palazzetti R, Minak G. The effect of interleaved composite nanofibrous mats on delamination behavior of polymeric composite materials. Compos. Struct. 2014; 109: 41–7. http://dx.doi.org/10.1016/j.compstruct.2013.10.039.

[34] A. Aksoy L.A. Carlsson. Interlaminar shear fracture of interleaved graphite/epoxy composites Compos. Sci. Technol. Volume 43, Issue 1, 1992, Pages 55-69.

[35] Jong W, Kim J and Seok L.Influence of Interleaved Films on the Mechanical Properties of Carbon Fiber Fabric/Polypropylene Thermoplastic Composites Materials 2016; 9: 344.

[36] Yu Y, Zhang Z, Gan W, Wang M and Li, S. () Effect of polyethersulfone on the mechanical and rheological properties of polyetherimide-modified epoxy systems. Industrial and Engineering Chemistry Research. 2003; 42: 3250–3256.

[37] Ying W, Bin Yang HS, Moon DS, Lee MW, Ko NY, Kwak NH, Lee B, Zhu J and Zhang R. Epoxy resins toughened with in situ azide-alkyne polymerized polysulfones. Journal of Applied Polymer Science. 2017; 135: 45790

[38] Si-Eun Lee Euigyung Jeong Man Young Lee Min-Kyung Lee Young-Seak Lee, Improvement of the mechanical and thermal properties of polyethersulfone-modified epoxy composites, Journal of Industrial and Engineering Chemistry Volume 33, 25 January 2016, Pages 73-79

[39] R. Rajasekaran, M. Alagar, C. Karikal Chozhan, Effect of polyethersulfone and N,N′-bismaleimido-4,4′-diphenyl methane on the mechanical and thermal properties of epoxy systems, eXPRESS Polymer Letters Vol.2, No.5 (2008) 339–348

[40] Mimura K, Ito H and Fujioka H. Improvement of thermal and mechanical properties by control of morphologies in PES-modified epoxy resins. Polymer. 2000; 41: 4451–4459.

[41] Anthony D, Bacarreza O, Shaffer MSP, Bismarck A, Robinson P, Pimenta S, Crack arrest in finger jointed thermoplastic pes interleaved CFRC 21st International Conference on Composite Materials Xi 2017.

[42] Kuboki T, Jar PYB and Forest TW. Influence of interlaminar fracture toughness on impact resistance of glass fibre reinforced polymers. Compos. Sci. Technol. 2003; 63: 943-953.

[43] Zhu DZ, Chen Q, Ma ZJ. Impact behavior and damage characteristics of hybrid composites reinforced by Ti fibers and M40 fibers. Materials & Design. 2015; 76: 196-201.

[44] Hung P, Lau K, Cheng L, Leng J, Hui D, Impact response of hybrid carbon/glass fiber reinforced polymer composites designed for engineering applications, Composites Part B. 2018; 133: 86-90.

[45] Remmers J. Discontinuities in materials and structures: a unifying computational approach. Delft University of Technology; 2008.

[48] Najafi M, Ansari R and Darvizeh A. environmental Effects on Mechanical Properties of Glass/Epoxy and Fiber Metal Laminates, Part I: Hygrothermal Aging. 2017; 7: 187-196

[47] Morinière F, Alderliesten R., Tooski M, Benedictus R. Damage evolution in GLARE fibre-metal laminate under repeated low-velocity impact tests. Central European Journal of Engineering 2012; 2: 603-611.

[48] Yaghoubi AS, Liu Y, Liaw B. Stacking sequence and geometrical effects on lowvelocity impact behaviors of GLARE 5 (3/2) fiber-metal laminates. J Thermoplast Compos Mater 2012; 25: 223–47.

[49] Laliberté JF, Straznicky PV, Poon C. Impact damage in fiber metal laminates, part 1: experiment. AIAA J 2005; 43: 2445–53.

[50] Morinière FD, Alderliesten RC, Benedictus R. Modelling of impact damage and dynamics in fibre-metal laminates – a review. Int J Impact Eng. 2014; 67: 27–38.

[51] Liu Y, Liaw B. Effects of constituents and lay-up configuration on drop-weight tests of fiber-metal laminates. Appl Compos Mater. 2009; 17: 43–62.

[52] Vlot A. Impact loading on fibre metal laminates. Int J Impact Eng 1996; 18: 291–307.

[53] Vlot A, Kroon E, La Rocca G. Impact response of fiber metal laminates. Key Eng Mater 1998; 141–143: 235–76.

[54] Laliberté JF, Straznicky PV, Poon C. Impact damage in fiber metal laminates, part 1: experiment. AIAA J 2005; 43: 2445–53.

[55] Zarei H, Fallah M, Minak G, Bisadi H, Daneshmehr AR. Low velocity impact analysis of Fiber Metal Laminates (FMLs) in thermal environments with various boundary conditions. Compos. Struct. 2016; 149: 170–83.

[56] Zarei H, Sadighi M, Minak G. Ballistic analysis of fiber metal laminates impacted by flat and conical impactors. Compos. Struct. 2017; 161: 65–72.

[57] ASTM D7136-Standard Test Method for Measuring the Damage Resistance of a Fiber-Reinforced Polymer Matrix Composite to a Drop-Weight Impact Event; 2005.

[58] Caprino G, Lopresto V, Scarponi C, and Briotti G, "Influence of material thickness on the response of carbon-fabric/epoxy panels to low velocity impact," Compos Sci Technol 1999; 59(15): 2279–2286.

[59] Schoeppner GA and Abrate S. "Delamination threshold loads for low velocity impact on composite laminates," Compos Part A Appl Sci Manuf 2000; 31(9), 903–915.

[60] Abisset E, Daghia F, Sun XC, Wisnom MR, and Hallett SR, "Interaction of inter- and intralaminar damage in scaled quasi-static indentation tests: Part 1 – Experiments," Compos. Struct., 2016; 136: 712–726.